Article

Optimization of Operating Parameters for Straw Returning Machine Based on Vibration Characteristic Analysis

Yuanyuan Gao [1,2] (ID), Yongyue Hu [1], Yifei Yang [1], Kangyao Feng [1], Xing Han [1], Peiying Li [3], Yongyun Zhu [1,2] and Qi Song [1,2,*]

1 School of Agricultural Engineering, Jiangsu University, Zhenjiang 212013, China;
   gaoyy0910@ujs.edu.cn (Y.G.); hy_0512@stmail.ujs.edu.cn (Y.H.); yyfjsdxyx@stmail.ujs.edu.cn (Y.Y.);
   kangyaofeng@stmail.ujs.edu.cn (K.F.); hanx1010@stmail.ujs.edu.cn (X.H.); yongyunzhu@ujs.edu.cn (Y.Z.)
2 Key Laboratory of Modern Agricultural Equipment and Technology, Ministry of Education,
   Zhenjiang 212013, China
3 College of Information and Electrical Engineering, China Agricultural University, Beijing 100083, China;
   sy20243081950@cau.edu.cn
* Correspondence: songqi@ujs.edu.cn

Abstract: For the mechanized technical mode of total wheat straw returning to field, there are problems such as large vibration during the operation of the straw returning machine that, in turn, affect the effect of stubble breaking. This study took the Tongtian 1-JHY-220 straw returning machine as the research object to conduct field experiments, with wheat stubble height, forward velocity, and PTO speed as experimental parameters. And the vibration characteristics at different positions of the machine and the final stubble breaking rate were used as evaluation indicators. Combined with the orthogonal experiment and response surface analysis method, this article analyzes and discusses the influence of various parameters on vibration characteristics and operational effectiveness. The results show that PTO speed and wheat stubble height were the main factors affecting the vibration and operation quality of the straw returning machine. Low PTO speed and high stubble height can improve the stubble breaking rate of the straw returning machine and reduce its operation vibration. Furthermore, the multi-objective optimization results show that when the forward velocity in the range of 8.5–9 km/h, the PTO speed is 540 r/min, and the stubble height is in the range of 200–250 mm, the stubble breaking rate of the straw returning machine is greater than 86%. At this time, the total vibration of the straw returning machine and tractor rear axle is relatively small. This study can lay a foundation for further studying the impact of the vibration of the straw returning machine on the stubble breaking effect and provide a reference for the preparation of high-quality seedbed under conservation tillage.

Keywords: conservation tillage; straw returning machine; vibration characteristic; stubble breaking rate; parameter optimization

1. Introduction

The Huang-Huai-Hai region belongs to the area of double cropping in one year. After wheat harvest, there is a large amount of stubble covering the ground that is difficult to handle in actual production, and it is necessary to carry out straw mulching operations in a timely manner to ensure the quality of no-tillage corn planter operation [1–3]. At the same time, straw mulching effectively diminishes soil erosion caused by wind and water, enhances soil fertility, and increases moisture retention [4]. Therefore, in recent years, the Ministry of Agriculture and Rural Affairs has begun to implement a large-scale mechanized technical mode of total wheat straw returning to the field in which the harvester harvests wheat with high stubble retention, and then the straw is mechanized in situ through the straw returning machine to crush and uniformly scattered on the ground. This conservation tillage technology has become an important means of arable land quality enhancement

and protection [5], which can greatly improve the effectiveness of straw mulching for the planting and growth of the next crop, and it has been widely promoted and applied in the wheat and jade rotational cropping area of the Huang-Huai-Hai plain. However, Chen et al. [6] conducted a comparative field experiment and measured the actual power consumption of the straw returning machine at 29.443 kW, which was 9.06% higher than the predicted value. The reason for this abnormal phenomenon is that, during field operation, the straw returner was susceptible to external excitation forces such as uneven ground surface and work resistance, resulting in severe vibration and high energy consumption [7]. Strong mechanical vibration not only causes a reduction in the reliability of the unit's operation and affects the driver's maneuverability [8] but also leads to a shorter time of trouble-free operation of the machine and a reduction in the quality of the operation [9]. Therefore, in order to achieve high reliability and high-quality operation of the straw returning machine, it is necessary to conduct a comprehensive study and analysis of the vibration and operational quality of the straw returning machine.

At present, many scholars have made some progress in the study of the vibration of the straw returning machine. For example, Zhao et al. [10] conducted simulation research on the casing and cutter roller shaft of the 1JH-185 straw returning machine and found that the casing is more prone to vibration during operation. Gao et al. [11] optimized the structure of the resonance part of the corn-straw deep-buried returning machine using finite element method, which improved the operational efficiency. Liu et al. [12] proposed a method of corn straw crushing and returning to the field using different speed rollers and dynamic double support forms by analyzing the dynamics of corn straw and the area of straw leakage during the operation, and a mathematical model was established to determine the impact on the qualified rate of straw crushing. Kazuaki et al. [13] investigated the influence of the forward velocity and cutter roller speed of the straw returning machine on the vibration of the rotary tiller blade and discovered that the vibration experienced by the rotary tiller blade intensifies as the forward velocity and rotational speed increase. Song et al. [14] used ANSYS 2016 software to conduct a finite element analysis on the blade shaft of the straw returning machine and found that the vibration frequency of the cutter roller shaft during operation was much lower than the minimum frequency within the natural frequency range, and no resonance phenomenon occurred. Researchers optimized the designed straw returning machines through a simulation analysis, mathematical modeling, and bench experiments and improved their motion parameters, structure, and even machinery [15–17]. The aforementioned study on the straw returning machine's vibration primarily concentrated on modal analysis and experimenting, as well as vibration bench experimenting. However, there is scant research on the operational vibration parameters of the straw returning machine.

On the other hand, the operating parameters of the straw returning machine can affect its vibration and operational effectiveness [18,19]. For this reason, scholars have studied the operating parameters of the straw returning machine, such as the wheat stubble height, forward velocity, and cutter roller speed. For example, the height of wheat stubble on farmland can affect the operation quality of straw returning machine [20]. Guo et al. [21] found that increasing the speed of the cutter roller of the straw returning machine can significantly improve the quality of straw mulching. Meanwhile, Zhang et al. [22] found that the higher the speed of the cutter roller, the greater the power consumption, which in turn increased machine vibration and noise. Zhao et al. [23] found that the forward velocity of the straw returning machine unit would affect the stubble breaking effect, and the faster the speed, the greater the vibration of machine and the worse the operation effect. These studies mostly focused on the influence of a certain parameter, lacking research on the combination of multiple operating parameters and different working conditions, and there are relatively few studies on the comprehensive analysis of the vibration and operating effects of the straw returning machine.

In response to the aforementioned issues, this paper aims to investigate the impact of operational parameters on the vibration and performance of the straw returning machine when operating in full wheat straw crushing mode, so field experiments were conducted using various combinations of operational parameters on the machine. The study analyzed the resulting vibration characteristics and operational outcomes and performed multi-objective optimization to identify the optimal set of operational parameters. The goal was to enhance the machine's operational performance to better satisfy the requirements for the straw returning machine and to offer guidance for the efficient management of wheat residue and the optimization of straw returning machine operations in the wheat straw-rotation region.

2. Materials and Methods

2.1. Straw Returning Machine's Structure and Working Principle

The straw returning and crushing machine's overall structure comprises a three-point hitch device, casing, cutter roller, and transmission device, along with a press roller. As depicted in Figure 1, the Dongfanghong LX-1804 tractor's (YTO Co., Ltd., Luoyang, China) power take-off (PTO) shaft will transfer power to the Tongtian 1JHY-220 straw returning machine's (Hebei Tongtian Machinery Co., Ltd., Shijiazhuang, China) gearbox via a universal joint to drive cutter roller.
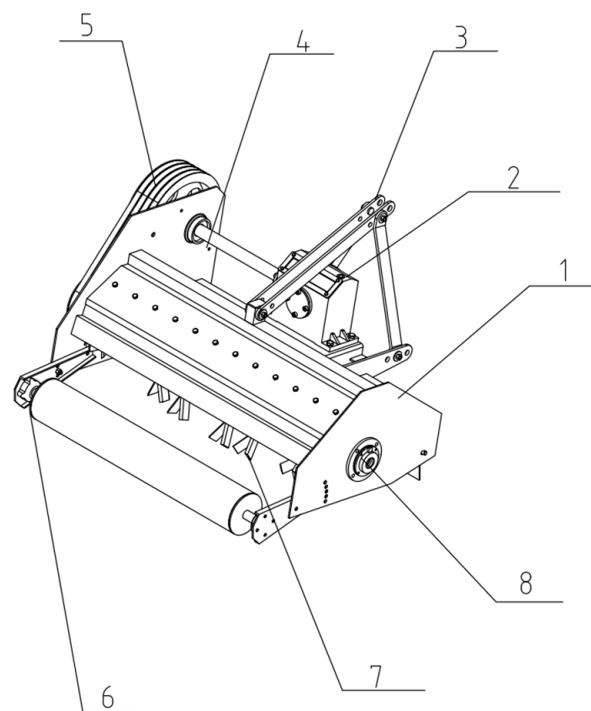
Figure 1. Structure of straw returning machine: (1) machine casing, (2) gearbox, (3) three-point hitch device, (4) side drive shaft, (5) belt, (6) press roller, (7) grinding blade, and (8) chopping shaft.

During operation, the straw returning machine should adjust its height according to the appropriate stubble height. It is recommended that the burial depth of the grinding blade during operation should not exceed 5 cm. Wheat stubble in the high-speed rotation of the grinding blade was cut and crushed; evenly dispersed on the ground; and then, via press roller grinding, stuck to the ground [24]. The related parameters of the operating unit are shown in Table 1.

Table 1. Related parameters of operating unit.

Tool Type	Parameters	Values/Styles
1JHY-220	Overall size (mm)	$1380 \times 2480 \times 1050$
	Structural weight (kg)	715
	Working width (m)	2.2
	Rotational speed of chopping shaft (r/min)	2160
	Maximum turning radius of cutting (mm)	255
LX-1804	Overall size (mm)	$5100 \times 2380 \times 3120$
	PTO speed (r/min)	540/720
	PTO power (kW)	112.5

2.2. Straw Returning Machine: Theoretical Analysis of Vibration Characteristics

The straw returning machine was rotatably connected to the tractor through a three-point hitch device. During field operations, the machine encountered disturbances caused by uneven terrain, varying working resistance, and external excitation forces from the tractor's rear output shaft, resulting in fluctuations in vertical displacement [11]. The autocorrelation functions of its vibrational characteristics were distributed as positive and cosine functions [25]. Assuming that the longitudinal undulating pattern of the working ground of the straw returning machine varied sinusoidally, a simplified vibration model of the field operation of the straw returning machine can be established, as depicted in Figure 2. In this model, the unit was subjected to a harmonic excitation from the external periodic variation in the excitation force. *M* represents the quality of the straw returning machine, kg; *K* is the spring stiffness of the system, N/m; *C* is the damping coefficient of the system; *T* is the wavelength along the working direction; and *A* is the vibration amplitude of the system relative to the ground, m.
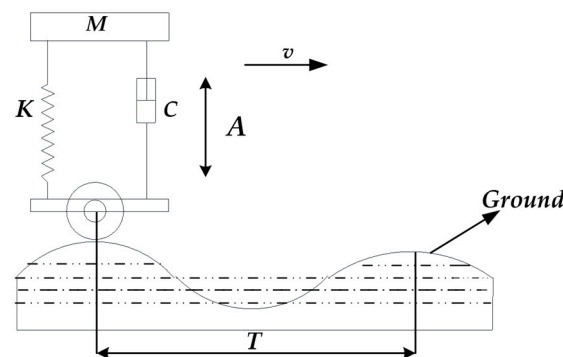
Figure 2. Vibration system model of field operation.

In order to facilitate the solution of the vibration system model of the straw returning machine and ignore the secondary influencing factors on the vibration of the machinery, the following assumptions are made before establishing the vibration mathematical model [26]. ① The casing, press roller, chopping shaft, and other components of the straw returning machine are rigid bodies. ② The spring stiffness of the grinding blades, the frame, and the press roller exhibits a linear relationship with displacement; meanwhile, the damping produced by the interaction of these various components is directly proportional to velocity. ③ The equipment has no lateral deviation movement.

The differential equation of motion for the harmonic excitation received by the straw returning machine is as follows:

$$M\ddot{A} + C\dot{A} + KA = F(t) = F_0 sinwt \tag{1}$$

$$\omega = 2\pi\frac{v}{T} \tag{2}$$

where F_0 is the external excitation force, and ω is the frequency of the excitation force.

The solution of differential Equation (1) consists of two parts: homogeneous general solution, A_1; and non-homogeneous specific solution, A_2. In the case of small damping, the general solution is a response to the initial conditions: attenuated vibration, also known as transient vibration. Generally, as time increases, the general solution, A_1, usually decays to a threshold close to zero; and the special solution, A_2, represents the forced vibration generated by the system under harmonic excitation, which is a continuous equal amplitude motion and a steady-state vibration. Therefore, when solving the steady-state vibration response of the straw returning machine in this paper, the influence of the general solution is generally ignored, and only the specific solution, A_2, is considered.

$$A_2 = A\sin(\omega t - \varphi) \tag{3}$$

$$a = -A\omega^2\sin(\omega t - \varphi) \tag{4}$$

where φ is the phase difference, and a is the vibration acceleration.

Substituting Equation (3) into the motion differential equation, Equation (1), results in the following.

$$\left(K - M\omega^2\right)A\sin\left(\omega t - \varphi\right) + C\omega A\cos\left(\omega t - \varphi\right) = F_0\sin\omega t \tag{5}$$

$$F_0\sin\omega t = F_0\cos\varphi\sin\left(\omega t - \varphi\right) + F_0\sin\varphi\cos(\omega t - \varphi) \tag{6}$$

$$\left\{\left(K - M\omega^2\right)X - \cos\varphi F_0\right\}\sin\left(\omega t - \varphi\right) + \left\{C\omega X - \sin\varphi F_0\right\}\cos\left(\omega t - \varphi\right) = 0 \tag{7}$$

We need to solve Equations (5) and (6) simultaneously. For Equation (7), its solution is always equal to 0; therefore we have Equations (8) and (9).

$$\left(K - M\omega^2\right)A - \cos\varphi F_0 = 0 \tag{8}$$

$$C\omega A - \sin\varphi F_0 = 0 \tag{9}$$

$$A = \frac{F_0}{\sqrt{\left(K - M\omega^2\right)^2 + (C\omega)^2}} \tag{10}$$

$$\varphi = \tan^{-1}\frac{C\omega}{\left(K - M\omega^2\right)} \tag{11}$$

$$\omega_n = \sqrt{\frac{K}{M}} \tag{12}$$

$$\tau = \frac{C}{2M\omega_n} \tag{13}$$

where ω_n is the fixed frequency of the system in an undamped state, and τ is the viscous damping coefficient of the system.

By substituting Equations (12) and (13) into Equations (10) and (11), the complete expressions for amplitude and phase difference can be obtained.

$$A = \frac{\frac{F_0}{K}}{\sqrt{\left\{1 - \left(\frac{\omega}{\omega_n}\right)^2\right\}^2 + 4\tau^2\frac{\omega^2}{\omega_n{}^2}}} \tag{14}$$

$$\varphi = \tan^{-1}\frac{\frac{2\tau\omega}{\omega_n}}{1 - \left(\frac{\omega}{\omega_n}\right)^2} \tag{15}$$

By combining the Equations (3) and (14) above, the solution to differential Equation (1) can be obtained.

$$A_2 = \frac{\frac{F_0}{K}}{\sqrt{\left\{1 - \left(\frac{\omega}{\omega_n}\right)^2\right\}^2 + 4\tau^2 \frac{\omega^2}{\omega_n{}^2}}} \sin(\omega t - \varphi) \tag{16}$$

$$a = \frac{\frac{F_0}{K}}{\sqrt{\left\{1 - \left(\frac{\omega}{\omega_n}\right)^2\right\}^2 + 4\tau^2 \frac{\omega^2}{\omega_n{}^2}}} \omega^2 \sin(\omega t - \varphi) \tag{17}$$

In the expression of forced vibration amplitude displacement and acceleration, in addition to system fixed factors such as stiffness, K; viscous damping coefficient, τ; and fixed frequency in an undamped state, ω_n, the forced vibration amplitude of the straw returning machine is also affected by the external excitation force, F_0, and excitation force frequency, ω. According to Equation (2), the excitation force frequency, ω, was related to the forward velocity (v) and wavelength (T) along the direction of operation, while the external excitation force, F_0, was affected by ground roughness and tractor output power. Our analysis shows that the vibration characteristics of the straw returning machine were influenced by factors such as the structural characteristics of the machinery, forward velocity, uneven ground, and PTO speed.

To this end, the experiment selected three parameters, namely PTO speed, forward speed, and stubble height, and studied their influence on the vibration characteristics of the straw returning machine, with a view to optimizing the operating parameters of the machine and improving the operating effect.

2.3. Filed Experiment Design of Straw Returning Machine

The experiment was conducted in June 2024 in the experimental field of Huimin County, Shandong Province. The high-stubble mode is limited to a range of no more than 250 mm, while the low-stubble pattern usually requires wheat stubble heights of less than 150 mm. So, before the experiment, we controlled the stubble height at three different heights of 150 mm, 200 mm, and 250 mm by adjusting the header height of the wheat harvester.

As shown in Figure 3, three-way acceleration sensors were installed on the straw returning machine and tractor, and each sensor was numbered, the specific numbers and locations of each measuring point were as follows: measuring point 1 (on the transmission shaft side of the upper shell of the straw returning machine), measuring point 2 (on the right side of the upper shell of the straw returning machine), measuring point 3 (on the bevel gear transmission box), measuring point 4 (near the left rear wheel of the tractor rear axle), and measuring point 5 (near the left rear wheel of the tractor rear axle). For the convenience of subsequent experimental data processing, during the experiment, the direction of the unit's movement was taken as the X direction, the direction perpendicular to the ground was taken as the Y direction, and the direction perpendicular to the forward velocity was taken as the Z direction. Therefore, the vibration experiment data at different positions of the unit were uniformly divided into three directions: X, Y, and Z.

This paper selected the wheat stubble height, the forward velocity of the unit, and the PTO speed of the tractor output shaft as experimental parameters. In order to accurately reflect the intensity of vibration at each measuring point, the root mean square (RMS) values of vibration acceleration were used as the evaluation standard [27]. Each experiment selected vibration experiment data from the stable working speed stage for 40 s. The three experimental parameters were denoted as X_1, X_2, and X_3, where X_1 and X_2 are 3-level factors, and the PTO speed, X_3, is a 2-level factor. The field orthogonal experimental plan is shown in Table 2.
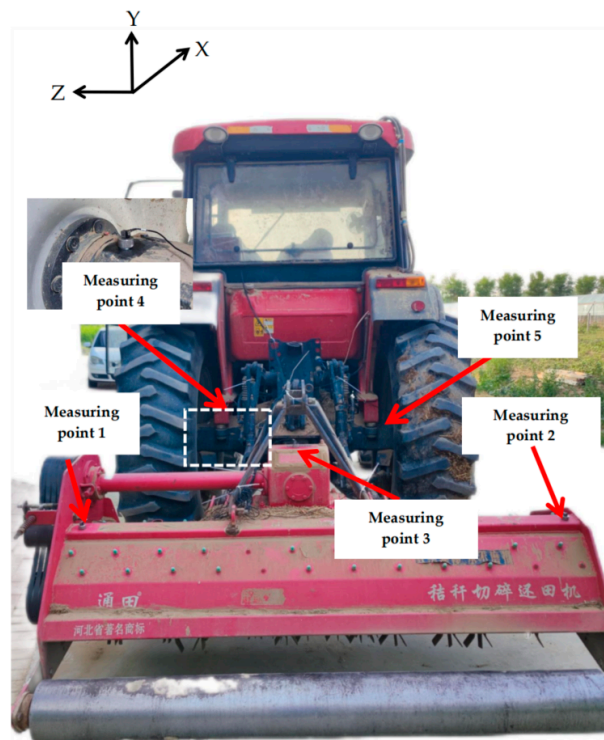
Figure 3. Distribution of each measuring point.

Table 2. Orthogonal field experiment table.

Number	Stubble Height, X_1 (mm)	Forward Velocity, X_2 (km/h)	PTO Speed, X_3 (r/min)
1	150	7.5	540
2	150	9	720
3	150	11	540
4	200	7.5	540
5	200	9	540
6	200	11	720
7	250	7.5	720
8	250	9	540
9	250	11	540

In order to reduce the influence of the tractor engine and transmission mechanism on signal acquisition and obtain the vibration effect of external excitation force during the operation of straw returning machine, a static vibration experiment was set as a blank control [28]. Specifically, the tractor was kept idle without load, and the tractor power output shaft was used to drive the straw returning machine for suspended no-load experiment, collecting vibration signals of the straw returning machine at three PTO speeds of 0 r/min, 540 r/min, and 720 r/min. Finally, vibration experiment data were selected for 12 s during the stable time period of each working condition. The data obtained from field experiments were subtracted from the static experiment data to obtain the corresponding vibration data.

2.4. Vibration Data-Acquisition Equipment

The equipment for collecting vibration characteristic information mainly included a dynamic signal analyzer, three-way acceleration sensors, and EDM 8.0 post-analyzer software. The experimental equipment is shown in Figure 4, and the operating parameters are shown in Table 3. Among them, Figure 4a shows a three-way acceleration sensor, model BWJ13533, and Figure 4b shows a Spider-80Xi dynamic signal analyzer (Crystal Instrument Company, Santa Clara, CA, USA). The data collected by the sensors were transmitted through the analyzer and then analyzed and processed by the EDM 8.0 post

analyzer software (Figure 4c). The sensors were attached to the metal surface of the desired experiment points via a magnetic suction base, as depicted in Figure 4d, to collect data on vibration acceleration and other parameters, thereby obtaining the vibration characteristics of the straw returning machine during field operations.

(**a**)

(**b**)

(**c**)

(**d**)
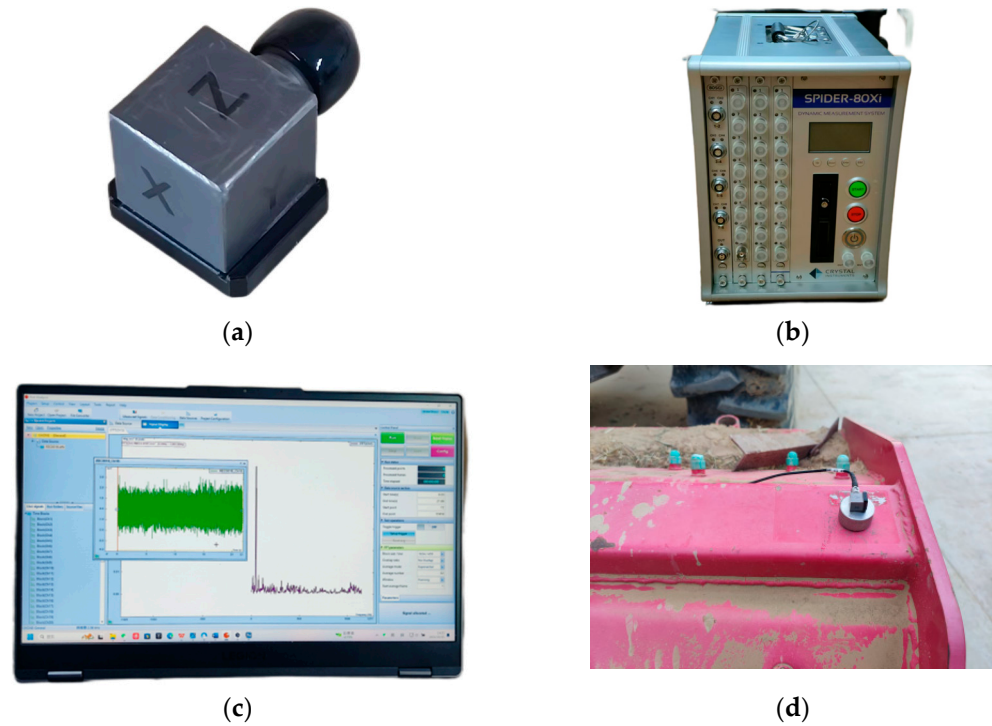
Figure 4. Experimental equipment: (**a**) three-way acceleration sensor, (**b**) spider-80Xi dynamic signal analyzer, (**c**) post-analyzer software, and (**d**) sensor installation diagram (measuring point 2).

Table 3. Main performance parameters of the experimental instruments.

Name	Parameters	Values/Styles
Spider-80Xi dynamic signal analyzer	Input channel	32
	Dynamic range (dB)	150
	Maximum sampling frequency (kHz)	102.4
Sensor type BWJ13533	Maximum sampling frequency (kHz)	6
	Sensitivity (mV/g)	50

According to the sampling theorem, the sampling frequency should be at least twice the analysis frequency [8]. Therefore, based on the analysis frequency of 1152 Hz, the sampling frequency was set to 2560 Hz, and the sampling method was continuous. Before the experiment, the 15 input channels of the Spider-80Xi dynamic signal analyzer must be enabled to collect vibration signal data [29]. When the machine's operating speed was stabilized near the target value in the experiment, the collection of machine vibration data began, with a sampling time of 40 s per group.

2.5. Evaluation Indicators

2.5.1. RMS Value

RMS reflects the strength of the signal and measures the variation in the random signal around the mean value, which in turn provides the basis for signal processing. To calculate the RMS values of a signal, we first should square and sum the vibration data at each

sampling point, then divide the sum by the number of sampling points, and take the square root [8,27]. The calculation formula is shown in Equation (18):

$$RMS = \sqrt{\frac{1}{N}\sum_{k=1}^{N}{x_k}^2} = \sqrt{\frac{{x_1}^2 + {x_2}^2 + {x_3}^2 + \cdots {x_k}^2}{N}} \tag{18}$$

where x_k is amplitude of vibration acceleration, m/s^2; and N is the number of signals collected.

As the vibration pattern of each measuring point varies depending on the distribution position and vibration source of each measuring point, the total vibration is used to feed back the vibration intensity [7]. The formula for calculating the total vibration is shown in Equation (19).

$$a_j = \sqrt{\frac{a_x^2 + a_y^2 + a_z^2}{3}} \tag{19}$$

where a_j is the total vibration of each measuring point, m/s^2; and a_x, a_y, and a_z represent the RMS values at the measuring points along the X, Y, and Z axes, m/s^2.

2.5.2. Stubble Breaking Rate

The stubble breaking rate is one of the evaluation indicators for the operation of the straw returning machine. In each of the experimental areas, three plots (50 cm × 50 cm) were randomly selected (as shown in Figure 5). All stubble within its range of surface and stubble depth was collected, dried, and sieved, and then the root stubble with a length greater than 50 mm and fibrous root mass were removed. The formula for calculating the stubble breaking rate is shown in Equation (20) [23]:

$$F_g = \frac{M_h}{M_z} \times 100(\%) \tag{20}$$

where F_g is stubble breaking rate, %; M_h represents the mass of roots with a length of less than 50 mm for both roots and whisker roots, g; and M_z represents total wheat stubble quality, g.

Figure 5. Wheat stubble cover.

3. Results

3.1. Analysis of Static Vibration Characteristics

The Dongfanghong LX-1804 tractor has a front engine and a PTO shaft; the PTO shaft is driven by the tractor engine, and the two speeds are proportional to each other. When the tractor drives the straw returning machine to operate at high speed, it will cause significant

vibration to the machine itself. The vibration data of each measuring point under static vibration are shown in Figure 6.

(**a**)

(**b**)

(**c**)

(**d**)

(**e**)
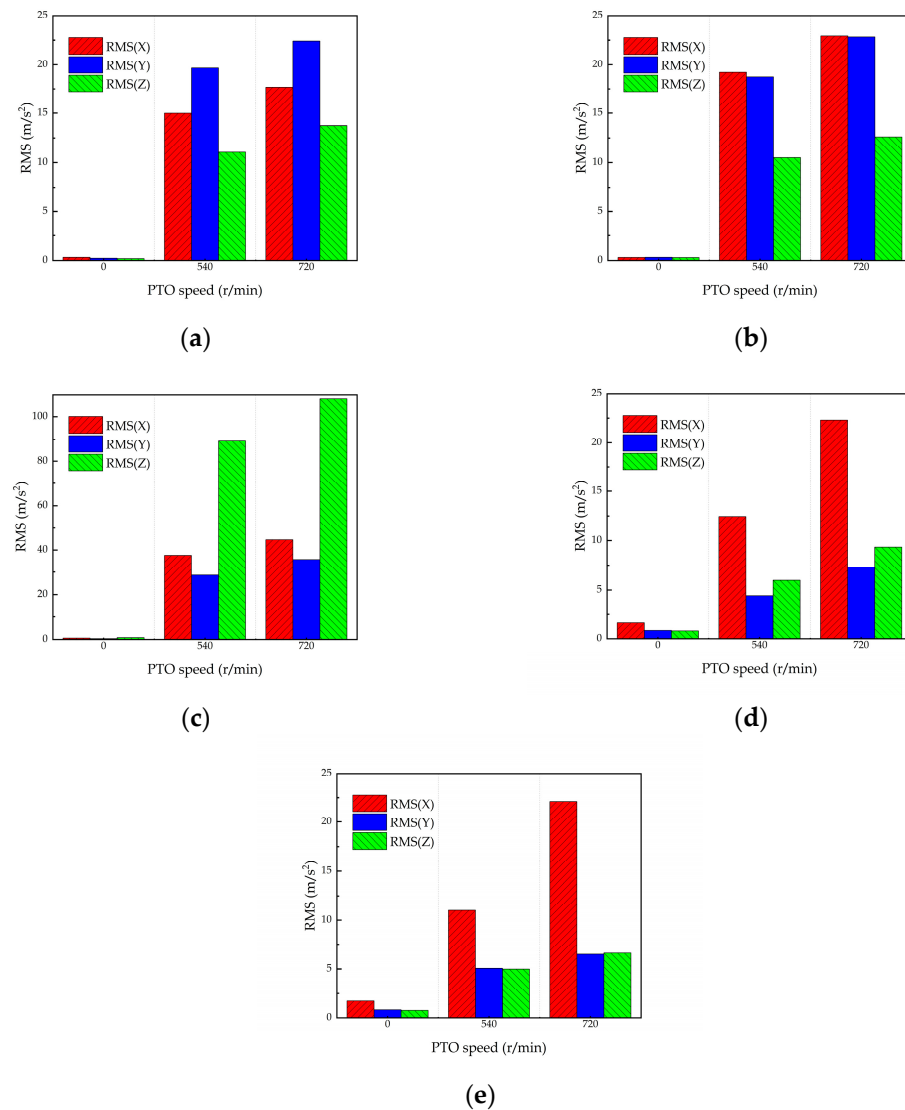
Figure 6. Vibration data of each measuring point under static vibration: (**a**) measuring point 1, (**b**) measuring point 2, (**c**) measuring point 3, (**d**) measuring point 4, and (**e**) measuring point 5.

As shown in Figure 6, most of the RMS values at each measuring point in all directions were less than 1, indicating that the tractor engine has little effect on the vibration of each measuring point when the tractor engine was idling.

When the PTO speed was at 540 r/min, the RMS values of each measuring point in all directions increased significantly, indicating that the PTO shaft of the tractor was one of the main vibration sources. The RMS values recorded for measuring points 1 and 2 in Figures 6a and 6b, respectively, hovered around the range of 10–15 m/s^2, and measuring point 3 displayed a remarkable Z-direction value of 82.6387 m/s^2, which underscored its significantly heightened vibration levels compared to measuring points 1 and 2 on the bevel gear transmission box. Consequently, it could be deduced that at measuring point 3, the directionality of the bevel gear transmission played a pivotal role in the pronounced lateral vibration, particularly influenced by the PTO speed [30].

When the PTO speed was at 720 r/min, there was a notable surge in vibration intensity across all orientations at the three measuring points of the straw returning machine. Specifically, measuring point 1 exhibited the most significant rise in lateral vibration, attaining

a magnitude of 77.6%; the lateral direction of measuring point 1 was greatly affected at high speeds by the side transmission device of the straw returning machine. However, the vibration of the other four measuring points was uniformly and significantly increased, and the vibration distribution pattern was consistent with that at 540 r/min.

In summary, it can be concluded that the PTO shaft is one of the main vibration sources of the straw returning returner, and a high-level PTO speed will intensify vibration.

3.2. Analysis of Dynamic Vibration Characteristics

Based on the RMS values' calculation results and stubble breaking rate, range and variance analyses were conducted on each parameter in the orthogonal experiment to obtain their impact weights on the experimental results. The RMS analysis results are shown in Tables 4 and 5, and the variance results of the stubble breaking rate are shown in Table 6.

Table 4. RMS range value of each measuring point under the influence of different parameters.

Measuring Point	Factor	Range (m/s^2)		
		X	Y	Z
1	Stubble height	2.261	6.298	5.711
	Forward velocity	3.827	12.217	5.24
	PTO speed	0.222	5.240	6.121
2	Stubble height	1.110	4.086	0.532
	Forward velocity	1.962	2.721	0.787
	PTO speed	6.163	3.618	3.9631
3	Stubble height	1.105	4.503	15.066
	Forward velocity	1.022	3.659	8.905
	PTO speed	14.23	0.866	16.532
4	Stubble height	3.404	0.766	0.771
	Forward velocity	0.345	0.127	0.906
	PTO speed	21.756	4.396	5.496
5	Stubble height	0.407	1.868	0.733
	Forward velocity	0.730	2.004	0.467
	PTO speed	8.496	3.440	2.813

Table 5. RMS analysis of variance for each measurement point.

Measuring Point	Factor	F-Ratios			*p*-Value		
		X	Y	Z	X	Y	Z
1	Stubble height	2.261	6.298	5.711	0.239	0.007 **	0.434
	Forward velocity	3.827	12.217	5.24	0.081	0.001 **	0.541
	PTO speed	0.222	5.240	6.121	0.837	<0.001 **	0.201
2	Stubble height	1.110	4.086	0.532	0.499	0.139	0.864
	Forward velocity	1.962	2.721	0.787	0.179	0.319	0.748
	PTO speed	6.163	3.618	3.9631	0.003 **	0.066	0.021 *
3	Stubble height	1.105	4.503	15.066	0.712	0.365	0.034 *
	Forward velocity	1.022	3.659	8.905	0.776	0.475	0.134
	PTO speed	14.23	0.866	16.532	0.001 **	0.734	0.008 **
4	Stubble height	3.404	0.766	0.771	0.019 *	0.128	0.192
	Forward velocity	0.345	0.127	0.906	0.824	0.891	0.137
	PTO speed	21.756	4.396	5.496	<0.001 **	<0.001 **	<0.001 **
5	Stubble height	0.407	1.868	0.733	0.617	0.572	0.104
	Forward velocity	0.730	2.004	0.467	0.307	0.571	0.322
	PTO speed	8.496	3.440	2.813	<0.001 **	0.119	0.001 **

Note: * indicates that the item is significant (F > $F_{0.05}$), ** indicates highly significant (F > $F_{0.01}$).

Table 6. Analysis of variance of stubble breaking rate.

Factor	Mean Square	DOF	F-Ratios	*p*-Value
Stubble height	42.658	2	1.361	0.38
Forward velocity	8.826	2	0.282	0.772
PTO speed	3.351	1	0.107	0.765
error	31.333	3	2	540

3.2.1. Analysis of Dynamic Vibration Characteristics of Straw Returning Machine

The orthogonal test can clarify the influence of each operating parameter on the vibration of the straw returning machine in order to obtain the influence weights of the PTO speed, stubble height, and forward speed on the straw returning machine. So, the three operating parameters were analyzed in detail in conjunction with Figure 7 and Tables 4–6. The following section discusses the three parameters in points.
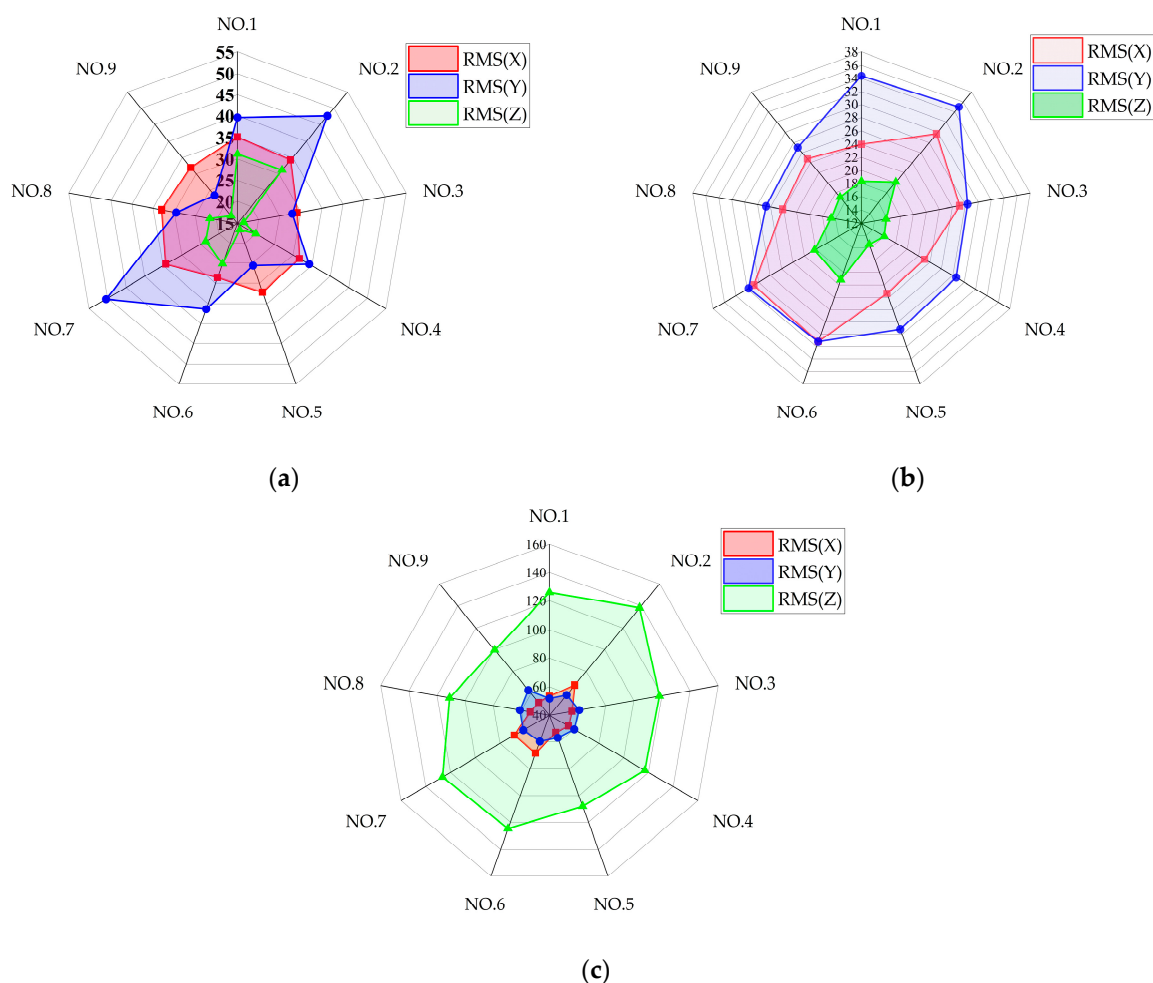
Figure 7. RMS values of the straw returning machine in the X, Y, and Z directions under various experimental conditions: (**a**) measuring point 1, (**b**) measuring point 2, and (**c**) measuring point 3.

(1) According to Tables 4 and 5 and Figure 7, it can be seen that the direction of acceleration changes in different parts of the straw returning machine during field operations was not consistent. Among them, the vibration acceleration values of each measuring point in the Z direction (horizontal) were ranked in the order of point 3 > point 1 > point 2, and they were more evenly distributed in the other two directions. Based on the results of the significance analysis, the PTO speed had a significant impact on measuring point 1 (Y direction) of the straw returning machine, and the layout of the transmission device on the

left side had a greater impact on the vibration of the machine. For measuring points 2 and 3, which were far away from the belt transmission, the PTO speed had a significant impact on the X and Z directions. The F-ratio of PTO speed to stubble breaking rate in Table 6 is only 0.107, which indicates that increasing the PTO speed did not significantly improve the stubble breaking rate; instead, it significantly increased the overall vibration.

Therefore, it can be inferred that the influence of PTO speed on the overall vibration of the straw returning machine was mainly on the X and Z directions, while there was no significant impact on the vertical direction.

(2) Upon examining Tables 4 and 5, it becomes evident that stubble height significantly influenced the vertical vibration at measuring points 1 and 2, with peak values reaching 6.298 m/s^2 and 4.086 m/s^2, and the horizontal vibration at measuring point 3 reached its maximum at 15.066 m/s^2. So, it can be concluded that the impact of stubble height on the straw returning machine was notably pronounced in the vertical direction at measuring point 1 and in the horizontal direction at measuring point 3, which suggested that the influence of stubble height on the machine's vibration was primarily focused on the left transmission assembly. In Table 6, the F-ratio comparing stubble height to stubble breaking rate is 1.361, the highest among the three parameters studied.

It can be inferred that stubble height indeed had a measurable effect on the stubble breaking rate, and increasing stubble height can both diminish the machine's vibration and enhance the quality of the operation.

(3) Every three sets of experiments had two identical PTO speeds and the same stubble height, with only the forward velocity of the unit operation being different. By comparing experiments 1 and 3, experiments 4 and 5, and experiments 8 and 9, the impact of forward velocity on operational vibration can be compared and analyzed. Based on the RMS values in Figure 7a,b, it can be seen that the X-direction acceleration of each measuring point did not increase significantly with the increase in forward velocity, and it even showed a decreasing trend in some comparison groups. Furthermore, based on Figure 5, the forward velocity had a significant impact on the vertical direction of measuring point 1, and it had no significant impact on all other measuring points in all directions. Combining this information with the F-ratio of forward velocity to stubble breaking rate in Table 6, which is only 0.282, it can be concluded that the forward velocity had no significant effect on the vibration and operation efficiency of the returning machine, indicating that higher or lower forward speeds have little effect on the operation efficiency of the straw returning machine.

Based on the comprehensive analysis of the abovementioned experimental results, the PTO speed and wheat stubble height are the main factors affecting the vibration and operation quality of the straw returning machine. Therefore, a low PTO speed and high stubble height can ensure a high level of stubble breaking rate, while also being beneficial for reducing the vibration.

3.2.2. Analysis of Dynamic Vibration Characteristics of Tractor

From the above analysis, it can be seen that the PTO speed was the main excitation source of the straw returning machine, and the rear axle of the tractor was close to the power output shaft, so this paper measured the vibration of the rear axle of the tractor in order to further study the effect of the PTO on the operation of the straw returning machine.

In Figure 8b, measuring points 4 and 5 have significantly higher X-direction acceleration values than the other two directions. In the significance analysis, the PTO speed had a significant impact on measuring points 4 and 5 in the X and Z directions, a result which is consistent with the pattern observed at measuring points 2 and 3. However, in Table 4, the maximum RMS value of measuring points 4 and 5 was only 21.756 m/s^2 in the X direction of measuring point 4. It can be concluded that the vibration distribution law of the tractor rear axle was consistent with that of the straw returning machine, but the rear axle vibration of the tractor was significantly smaller than that of the straw returning machine.

(a)   (b)
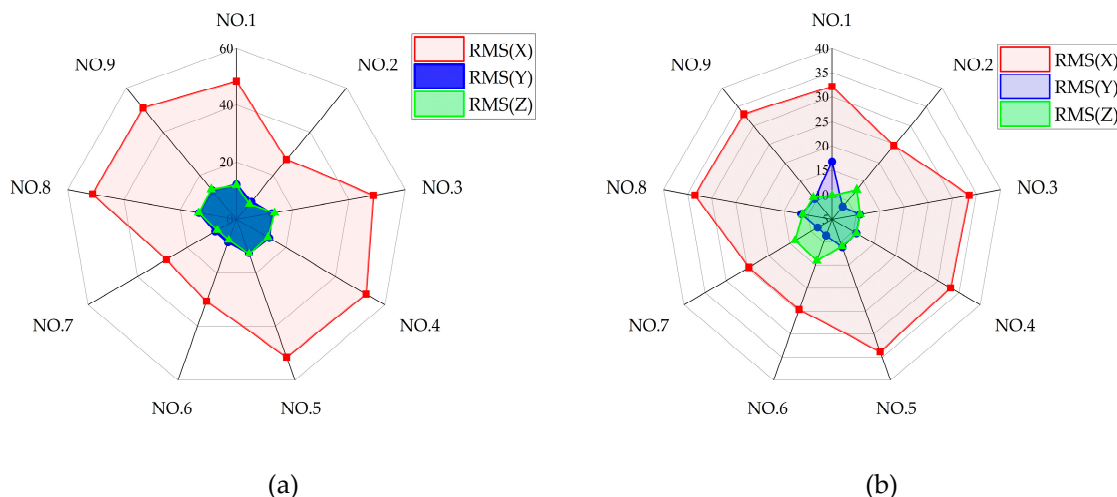
Figure 8. RMS values of the tractor rear axle in X, Y and Z directions under various experiment conditions: (**a**) measuring point 4 and (**b**) measuring point 5.

From Figure 8, it can be seen that when the PTO speed was at 720 r/min in experiments 2, 6, and 7, the maximum acceleration values in the X direction at measuring points 4 and 5 were 30.6076 m/s^2 and 24.6743 m/s^2, respectively. In the other six experimental conditions, the acceleration values of measuring points 4 and 5 in the X direction were significantly higher than those in experiments 2, 6, and 7 and were close to the acceleration values of the three measuring points in the Z direction. For the Y and Z directions, where the acceleration values of the two measuring points were relatively small, the acceleration variation pattern remained consistent with the X direction.

We analyzed the power spectral density (PSD) of measuring points 4 and 5 [31], and the results are shown in Table 7. It can be concluded that when the PTO speed was 540 r/min, the peak frequency of vibration at measuring points 4 and 5 was mainly concentrated around 40 Hz, while the PTO speed increased at 720 r/min, and the peak frequency of vibration was concentrated between 43 and 44 Hz. The peak power spectrum at low PTO speeds was generally smaller than at high PTO speeds, indicating that high PTO speeds could increase the amplitude of the tractor rear axle [32].

Table 7. Peak power spectra of measuring points 4 and 5 in the X direction.

Number	Point 4—X Direction		Point 5—X Direction	
	Peak Frequency (Hz)	Peak Power Spectrum (dB)	Peak Frequency (Hz)	Peak Power Spectrum (dB)
1	40.05	8.972	40.42	10.3
2	43.96	11.17	43.71	13.37
3	39.8	7.831	40.17	8.928
4	40.05	9.52	40.17	10.44
5	40.05	9.342	40.29	10.72
6	43.59	11.02	43.59	13.19
7	43.59	10.14	43.83	12.87
8	40.05	10.03	40.17	11.33
9	40.17	10.06	40.05	11.3

The reason for this abnormal phenomenon may be that the resonant frequency of the tractor rear axle body itself was around 40 Hz, and when the PTO speed was 540 r/min, the vibration source frequency of the tractor transmission mechanism was at the same level as the resonant frequency of the rear axle body, thus increasing the vibration of tractor measuring points 4 and 5.

Upon analyzing the data, it was evident that the vibration distribution pattern of the tractor's rear axle aligns with that of the straw returning machine, suggesting that the vibra-

tion experienced by both were influenced by the tractor engine's excitation, predominantly in their forward direction. This can be attributed to the fact that a lower PTO speed can effectively diminish the vibration in both the tractor and the straw returning machine.

3.3. Straw Returning Machine: Optimization of Operation Parameters

The multiple regression analysis can be used to explore the impact of multiple independent variables on a response variable. When dealing with nonlinear relationships, nonlinear regression models can more accurately capture complex relationships between variables and explore optimal combinations through multiple regression equation solutions. The results of the orthogonal experiment show that during the operation of the unit, the vibration of the tractor rear axle was significantly smaller than that of the straw returning machine.

Therefore, in order to clarify the influence of key operating parameters on the vibration characteristics and stubble breaking rate of the straw returning machine and optimize the parameter combination, multiple regression nonlinear equations were established, with the total vibration and stubble breaking rate of each measuring point as the response variables of the regression linear equation, using wheat stubble height, X_1; forward velocity, X_2; and PTO speed, X_3, as independent variables. X_1 and X_2 are encoded with +1, 0, and −1 to represent high, medium, and low levels, respectively, while X_3 is encoded with two levels and −1 and 1 to represent high and low levels. The experimental parameters and coding levels are shown in Table 8.

Table 8. Orthogonal experimental parameters and levels.

Variable	Parameters	Coding Level		
		−1	0	1
X_1	Stubble height (mm)	150	200	250
X_2	Forward velocity (km/h)	7.5	9	10.5
X_3	PTO speed (r/min)	540		720

3.3.1. Establishing Multiple Regression Equations

The total vibration of each measuring point and the results of each experiment's stubble breaking rate are shown in Table 9.

Table 9. Total vibration and stubble breaking rate under 9 experiments.

No.	Total Vibration at the Measuring Points (m/s^2)			Stubble Breaking Rate (%)
	Point 1	Point 2	Point 3	
1	35.488	26.443	84.474	85.546
2	38.377	28.936	95.067	81.165
3	25.197	24.416	83.388	78.471
4	29.340	23.129	82.442	80.281
5	25.595	23.342	76.845	89.145
6	30.415	28.255	89.183	90.581
7	37.748	28.106	90.197	88.371
8	28.418	22.902	79.425	93.145
9	24.940	23.35	74.38	85.880

The regression nonlinear module in IBM SPSS Statistics 26 software was used to find the parameter estimates of the total vibration and stubble breaking rate of the three measuring points and to investigate their regression coefficients. The regression equations of the total of vibration are in the form of Equation (21), and the regression equation of the stubble extinction rate is shown in the form of Equation (22).

$$y = a + bX_1 + cX_2 + dX_3 + eX_1X_2 + fX_1X_3 + gX_2X_3 \tag{21}$$

$$Y = a + bX_1 + cX_2 + dX_3 + eX_1^2 + fX_2^2 + gX_1X_3 + hX_2X_3 \qquad (22)$$

The results of obtaining the nonlinear variance coefficients for regression are shown in Table 10.

Table 10. Parameters table of regression equations.

Coefficients	Total Vibration (m/s²)			Stubble Breaking Rate (%)
	Point 1	Point 2	Point 3	
a	32.016	26.273	85.703	86.715
b	−1.919	−0.806	−3.362	7.36
c	−4.264	−0.176	−1.901	3.78
d	4.207	2.526	5.309	1.158
e	2.129	1.099	−1.411	5.791
f	−0.235	0.669	−0.693	6.907
g	−1.544	−0.367	0.072	4.715
h				6.268
Residual error	13.546	0.897	17	7.545
Corrected total sum	228.115	49.861	355.396	200.311
R^2	0.941	0.982	0.952	0.9622
R	0.9700	0.991	0.9757	0.9808

In the most significant case, for the solved equations, the critical value of R is 0.937. The R values of the regression equations for each measuring point in Table 10 are all greater than 0.937, indicating that the established nonlinear regression equations fit the total vibration and stubble breaking rate very well.

3.3.2. Response Surface Analysis

The response surface methodology is used to find the optimal conditions in multifactor systems, overcoming the disadvantage of only analyzing a single isolated experimental point in orthogonal experiments and not being intuitive enough, which has been widely applied in the parameter optimization of various experiments [33,34]. The total vibrations of measuring point 1 and the stubble breaking-rate regression equations were matrixed in ORIGIN 2024 software to obtain the response surface, and the effects of each experiment parameter on vibration and operation quality were analyzed, respectively.

For the total vibration at measuring point 1, the interaction response surface of the stubble height and forward velocity of the straw returning machine when the PTO speed was at 540 r/min is as shown in Figure 9a. The total vibration has a tendency to decrease with the increase in stubble height and forward velocity, and the main factor affecting the total vibration is stubble height in the interaction between forward speed and stubble height. When the stubble height was 200 mm, the interaction response surface between the forward velocity and PTO speed is shown in Figure 9b. As the PTO speed increased, the total vibration of measuring point 1 significantly increased, proving that PTO had a significant impact on the vibration of the straw returning machine and verifying the results of the orthogonal analysis in the previous text.

For the stubble breaking rate, Figure 10a shows, the interaction response surface of stubble height and the forward velocity when the PTO speed was 540 r/min. When the forward velocity is certain, the stubble breaking rate with the increase in the stubble height is first reduced and then increased, and the optimal stubble height is in the range of 220–250 mm. When the forward velocity is within the range of 8.5–9.5 km/h and the stubble height is in the range of 200–250 mm, the stubble breaking rate tends to reach its peak. In the interaction between forward velocity and stubble height, the main factor affecting the stubble extinction rate was stubble height.

(**a**)   (**b**)
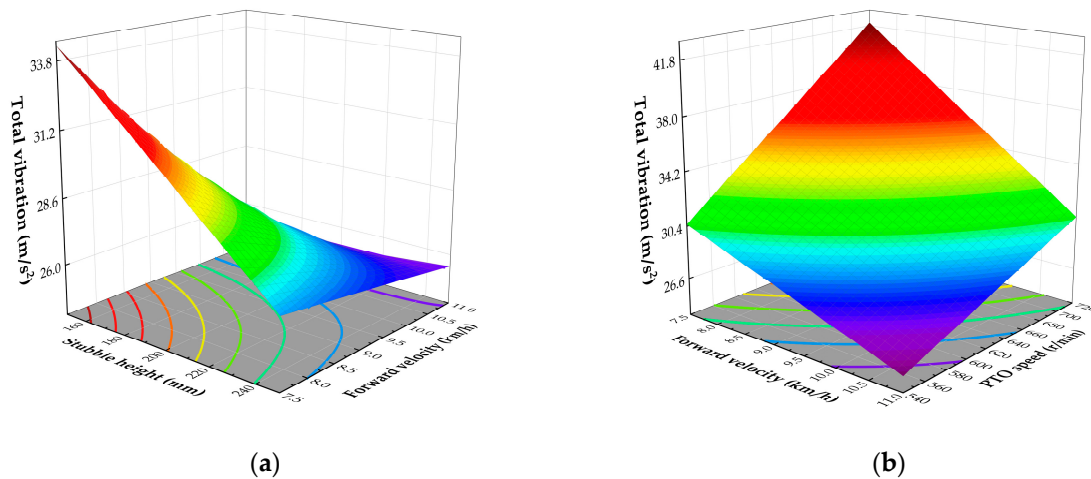
Figure 9. Total vibration response surface of measuring point 1: (**a**) PTO speed at 540 r/min and (**b**) stubble height at 200 mm.

(**a**)   (**b**)
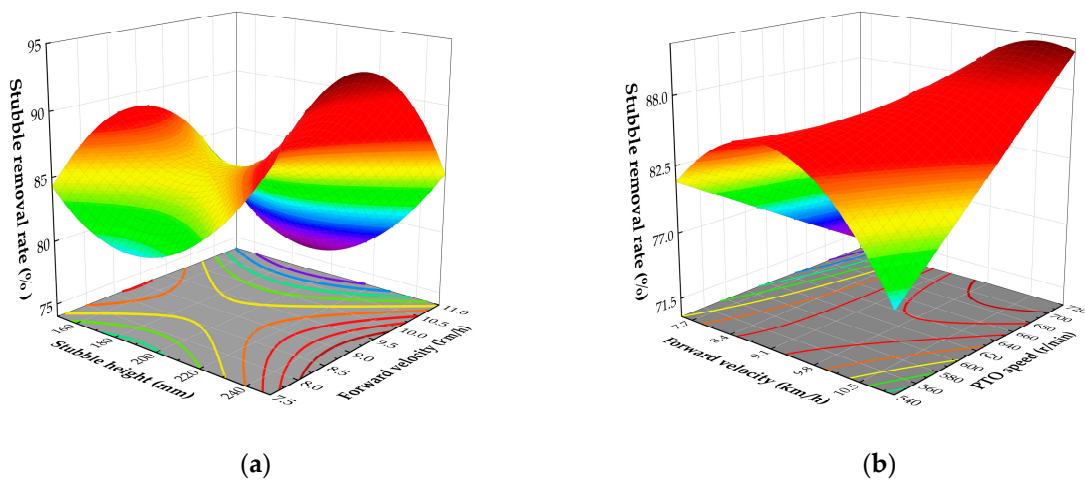
Figure 10. Response surface of stubble breaking rate: (**a**) PTO speed 540 r/min and (**b**) stubble height at 200 mm.

The interaction response surface between the PTO speed and the forward velocity of the straw returning machine is shown in Figure 10b for when the stubble height is 200 mm When the PTO speed is within the range of 540–560 r/min and the forward speed is between 8.5 and 9.5 km/h, the stubble breaking rate is at a high level, and when the PTO speed is within the range of 700–720 r/min and the forward velocity is within the range of 8.5–11 km/h, the stubble breaking rate is at high level.

The comprehensive response surface-analysis results show that the PTO speed and wheat stubble height are the main factors affecting the vibration and operation quality of the straw returning machine. A low PTO speed and high stubble height can improve the stubble breaking rate of the straw returning machine and reduce its operation vibration. This is consistent with the orthogonal test results.

3.4. Parameter Optimization and Validation

The purpose of optimizing the working and structural parameters of the machinery is to obtain the optimal parameters combination. Using the optimal function optimization module of MATLAB R2022a software, the nonlinear equations for the regression of total vibration and stubble breaking rate at the measuring point 1 and the measuring point 3 were selected to optimize the regression models by imposing constraints on the experimental parameters, in accordance with the working conditions of the straw returning machine and

the requirements of operational performance. The constraints for solving the experiment parameters are in the following equations:

$$max\ Y(x_1, x_2, x_3)$$

$$min y_1(x_1, x_2, x_3)$$

$$min y_3(x_1, x_2, x_3)$$

$$s.t. \begin{cases} 150\ \text{mm} < x_1 < 250\ \text{mm} \\ 7.5\ \text{km/h} < x_2 < 11\ \text{km/h} \\ x_3 = 540\ \text{r/min}\ or\ x_3 = 720\ \text{r/min} \end{cases}$$

Because the wheat stubble height cannot be changed during the process of returning to the field, it is necessary to select the optimal forward velocity and PTO speed based on the height of the wheat stubble. Therefore, by stepping the height of stubble by 5 mm, while maximizing the stubble breaking rate of the machinery and minimizing vibration, we obtain the optimal results are, as shown in Table 11.

Table 11. Optimization results of regression nonlinear equations.

X_1 (mm)	X_2 (km/h)	X_3 (r/min)	Y (%)	Total Vibration (m/s^2)	
				y_1	y_2
250	8.655	540	93.9491	27.4036	25.7396
245	8.6901	540	93.5573	27.6374	25.7013
240	8.6793	540	92.7887	27.8371	25.5991
235	8.7441	540	93.9662	28.2258	25.6571
230	8.75235	540	91.7192	28.5544	25.6325
225	8.7468	540	90.8844	28.8968	25.6049
220	8.74425	540	90.0466	29.2875	25.6048
215	8.9004	540	89.6610	30.1088	25.9035
210	8.9355	540	88.7541	30.6988	26.0092
205	8.97045	540	87.7735	31.3397	26.1355
200	9.00555	540	86.7193	32.0315	26.2823
195	7.5	540	85.5291	30.9103	23.8134
190	7.5	540	85.4790	31.2916	24.0708
185	7.5	540	85.4065	31.6729	24.3282
180	7.5	540	85.3116	32.0542	24.5856
175	7.5	540	85.1945	32.4355	24.8430
170	8.6455	720	80.9115	39.1899	29.1653
165	8.4237	720	80.8766	40.5352	29.3991
160	9.3812	540	75.6361	28.3130	24.7958
155	9.428	540	73.9195	28.3325	24.9037
150	9.4768	540	72.1292	28.3420	25.0065

From the analysis of the optimization results, it can be concluded that when the wheat stubble height is in the range of 200–250 mm, the stubble breaking rate of the machine could be above 86% at an operating speed of at range of 8.5–9 km/h and PTO speed of 540 r/min, thus meeting the operating standards.

4. Discussion

In full wheat straw-crushing mode, the combined harvester needs to carry out high stubble treatment on wheat straw, with a stubble height in the range of 15–25 cm. On the other hand, some scholars have found that the forward speed and PTO speed significantly affect the operational effect and vibration. Therefore, this article took the straw returning machine as the research object to conduct field experiments, with wheat stubble height, forward velocity, and PTO speed as experimental parameters. At the same time, the

vibration characteristics at different positions of the unit and the final stubble breaking rate were used as evaluation indicators.

This article combined the results of orthogonal experiments and response surface analysis to conclude that the PTO speed and wheat stubble height were the main factors affecting the vibration and operational quality of the straw returning machine. Furthermore, a low PTO speed and high stubble height can improve the stubble breaking rate and reduce the vibration. This finding aligned with the conclusions of other similar studies [20,22], which indicated that a higher level of wheat stubble height facilitated a more effective crushing treatment. However, it was also noted that the increase in stubble height led to greater working resistance [20], which in turn affected the vibration of the straw returning machine.

Our further analysis revealed that PTO had a significant impact on the overall vibration of the straw returning machine, but a high PTO speed did not significantly improve the stubble breaking rate; instead, it exacerbated the overall vibration. And here is another important point: the impact of stubble height on vibration primarily occurred at the chopping shaft and transmission device. This phenomenon arose because, as the stubble height increased, the soil obstruction to the chopping shaft during stubble breaking diminished, leading to a reduction in the vibration amplitude of the returning machine. This finding was consistent with the conclusion of Gao et al. [24], who suggested that the interaction between chopping shafts and soil was the main factor affecting the vibration of the straw returning machine throughout experiments.

This raised aspect had not been adequately addressed in previous studies on wheat stubble-returning treatments. Therefore, we suggested that during the wheat harvest stage, a relatively high stubble height could be appropriately retained. This approach would allow the straw returning machine to operate at a lower PTO speed, ensuring a high stubble breaking rate while reducing machine vibration. At the same time, it should be noted that this study had some limitations. The tractor selected for this study had a PTO speed that only included two modes, 540 and 720 r/min, since the PTO type of tractor is not easily changeable after leaving the factory. Therefore, the PTO speed could only be set to high or low during the actual experiments to assess its influence on the test results. Future research should consider the interaction effects of the PTO speed and stubble height at more levels to achieve optimal operational outcomes. Additionally, due to the similarity of experimental factors, the results of this study can also serve as a reference for optimizing the operating parameters of wheat combine harvesters.

In addition, a multi-objective optimization analysis was conducted on the total vibration and stubble breaking rate of the straw returning machine. The results indicated that when the forward speed was maintained between 8.5 and 9 km/h, with a PTO speed of 540 r/min and a stubble height ranging from 200 to 250 mm, the final stubble breaking rate was significantly improved, meeting operational standards. At this configuration, the total vibration (measuring points 1 and 3) was relatively low. Furthermore, for stubble heights within the range of 175–200 mm, a forward speed of 7.5 km/h and a PTO speed of 540 r/min should be selected, as the stubble breaking rate and total vibration are comparable to operational standards. It needs to be emphasized that when the stubble height falls within the range from 150 to 175 mm, the driver can increase the stubble breaking rate by increasing the PTO speed or decreasing forward speed; however, this adjustment results in a relatively higher vibration. In conclusion, it can be inferred that when the forward speed was within the range from 8.5 to 9 km/h, with a PTO speed of 540 r/min and stubble height between 200 and 250 mm, the stubble breaking rate was significantly enhanced, and the performance of straw returning machine remained stable. Additionally, the results of our field experiments, response surface theory analysis, and optimization equations are consistent and superior to the basic indicators.

This study has some limitations in that we ignored the vibration of the three-point suspension and the tractor drive points. And the vibration measurements were primarily taken from the casing of the straw returning machine. So, further research is needed

to explore the overall impact of the operating parameters on the unit and prioritize the overall operational requirements of the joint operation unit. In particular, we should directly measure the vibration of the vibration sources of the straw returner, including the transmission, the three-point suspension system, and the chopping shaft. Further, in this way, a comparative analysis with existing experiments will help identify the operating-parameter combinations for unit operation. In conclusion, it is essential to investigate the overall vibration and operational effects, integrating the complete process of crushing and returning of wheat stubble into the wheat joint operation equipment's workflow. This approach will provide valuable technical support for the development of conserving cultivation and the optimization of operational parameters.

5. Conclusions

At the mechanized technical mode of wheat straw returning to field, there are problems such as large vibration during the operation of the straw returning machine, affecting, in turn, the effect of stubble breaking. This study conducted field experiments on the straw returning machine using different combinations of operating parameters and analyzed the influence of each parameter on vibration characteristics and operating effects. Additionally, multi-objective optimization was performed under various stubble heights to determine the optimal operating parameters for the straw returning machine.

Combining the results of orthogonal experiments and response surface analysis, this article concludes that the PTO speed and wheat stubble height were the main factors affecting the vibration and operation quality. A further analysis led to the conclusion that a low PTO speed and high stubble height can improve the stubble breaking rate and reduce the vibration. This had an important guiding value for the selection of parameters for the mechanized technical mode of the straw returning machine. At the same time, multi-objective optimization solutions were carried out, and we deduced that appropriate forward speeds and PTO speeds should be selected for different stubble heights. The optimization results indicated that when the forward speed was within the range from 8.5 to 9 km/h, with a PTO speed of 540 r/min and stubble height between 200 and 250 mm, the stubble breaking rate was significantly enhanced, and the performance of the straw returning machine remained stable. This configuration also led to a corresponding reduction in the power consumption requirements of the tractor.

Although this study conducted field experiments under various operating parameters, there are limitations related to the selection of the tractor PTO speed and the arrangement of measuring points. Consequently, the identification of the optimal combination of operating parameters requires further refinement. Future research should concentrate on exploring a broader range of combinations of PTO speed and stubble height. This will allow for a more comprehensive investigation into the interaction effects of the overall vibration of the wheat combined operation unit and its operational performance. Ultimately, the objective is to improve the efficiency of wheat stubble breaking and ensure its efficient return to the field.

Author Contributions: Conceptualization, Y.G. and Q.S.; methodology, Y.G., Y.H., Y.Y. and K.F.; software, Y.Y. and Y.H.; validation, Y.G., Y.Y. and Y.H.; formal analysis, Y.G., Y.H. and Y.Y.; investigation, Y.G., Y.H., Y.Y., K.F. and X.H.; resources, Y.G. and Q.S.; data curation, Y.Y., Y.H. and P.L.; writing—original draft preparation, Y.G. and Y.H.; writing—review and editing, Q.S., Y.G. and Y.Z.; visualization, K.F., X.H. and P.L.; supervision, Y.G. and Y.Z.; project administration, Q.S. and Y.G.; funding acquisition, Y.G. All authors have read and agreed to the published version of the manuscript.

Data Availability Statement: The original contributions presented in the study are included in the article. Further inquiries can be directed to the corresponding author.

Conflicts of Interest: The authors declare no conflicts of interest.

References

1. Luo, X.; Liao, J.; Hu, L.; Zang, Y.; Zhou, Z. Improving agricultural mechanization level to promote agricultural sustainable development. *Trans. Chin. Soc. Agric. Eng.* **2016**, *32*, 1–11. [CrossRef]
2. Wang, Q.; Cao, X.; Wang, C.; Li, H.; He, J.; Lu, C. Research progress of no/minimum tillage corn seeding technology and machine in northeast black land of China. *Trans. Chin. Soc. Agric. Mach.* **2021**, *52*, 1–15. [CrossRef]
3. Lu, C.; Luo, X.; Li, H.; Zang, Y.; Ou, Y. Progress and suggestions of conservation tillage in China. *Strateg. Study Chin. Acad. Eng.* **2024**, *26*, 103–112. [CrossRef]
4. Yin, H.; Zhao, W.; Li, T.; Cheng, X.; Liu, Q. Balancing straw returning and chemical fertilizers in China: Role of straw nutrient resources. *Renew. Sustain. Energy Rev.* **2018**, *81*, 2695–2702. [CrossRef]
5. Wu, F.; Xu, H.; Gu, F.; Chen, Y.; Shi, L.; Hu, Z. Improvement of straw transport device for straw-smashing back-throwing type multi-function no-tillage planter. *Trans. Chin. Soc. Agric. Eng.* **2017**, *33*, 18–26. [CrossRef]
6. Chen, L.; Liang, X.; Cao, C. Virtual simulation and power test of straw counters-field based on multi-body dynamics. *Trans. Chin. Soc. Agric. Eng.* **2016**, *47*, 106–111. [CrossRef]
7. Chen, Y.; Tian, F.; Yan, Y.; Song, Z.; Li, F.; Chen, W. Development overview and analysis of tillage machinery abroad. *J. Chin. Agric. Univ.* **2018**, *39*, 7–11. [CrossRef]
8. Xu, L.; Chai, X.; Gao, Z.; Li, Y.; Wang, Y. Experimental study on driver seat vibration characteristics of crawler-type combine harvester. *Int. J. Agric. Biol. Eng.* **2019**, *12*, 90–97. [CrossRef]
9. Ma, Y.; Chen, Y. Nonlinear dynamic research on gear system with cracked failure. *J. Mech. Eng.* **2011**, *47*, 84–90. [CrossRef]
10. Zhao, X.; Ran, W.; Huo, X.; Liu, S.; Yu, H. Analysis on vibration characteristics of the straw returning machine. *J. Agric. Univ. Hebei* **2023**, *46*, 102–110. [CrossRef]
11. Gao, W.; Lin, J.; Li, B.; Wang, W.; Gu, S. Vibration characteristics analysis and structural optimization of straw deep bury and returning machine. *J. Jilin Univ.* **2022**, *52*, 970–980. [CrossRef]
12. Liu, P.; He, J.; Li, Y.; Li, H.; Wang, Q.; Lu, C.; Zhang, Z.; Li, S. Design and experiment of double rollers maize stalk chopping device with different rotation speeds. *Trans. Chin. Soc. Agric. Eng.* **2020**, *36*, 69–79. [CrossRef]
13. Hirasawa, K.; Kataoka, T.; Kubo, T. Relationship between required power and PTO speed in rotary tiller. *IFAC Proc. Vol.* **2013**, *46*, 141–146. [CrossRef]
14. Song, J.; Lin, J.; Ma, T.; Lv, L.; Tian, Y. Design of rotary shovel type corn straw deep buried returning machine. *J. Agric. Mech. Res.* **2018**, *40*, 95–99. [CrossRef]
15. Kumari, K.; Anand, K.; Bellacci, M.; Giannozzi, M. Effect of microstructure on abrasive wear behavior of thermally sprayed WC–10Co–4Cr coatings. *Wear* **2010**, *268*, 1309–1319. [CrossRef]
16. Liu, P.; He, J.; Zhang, Z.; Lu, C.; Zhang, Z.; Lin, H. Kinematic characteristic analysis and field experiment of chopped stalk in straw retention machine based on CFD-DEM coupling simulation method. *Trans. Chin. Soc. Agric. Mach.* **2020**, *51*, 244–253. [CrossRef]
17. Zhao, J.; Wang, X.; Zhuang, J.; Liu, H.; Wang, Y.; Yu, Y. Coupled bionic design based on primnoa mouthpart to improve the performance of a straw returning machine. *Agriculture* **2021**, *11*, 775. [CrossRef]
18. Gu, F.; Hu, Z.; Chen, Y.; Wu, F. Development and experiment of peanut no-till planter under full wheat straw mulching based on "clean area planting". *Trans. Chin. Soc. Agric. Eng.* **2016**, *32*, 15–23. [CrossRef]
19. Wang, Q.; Wang, Z.; Zhang, Z.; Zhang, K.; Yao, S.; Zhou, W.; Sun, X.; Wang, J. Design and Test of Bionic Elastic Row Cleaner with Improved Straw Cleaning Performance. *Agriculture* **2024**, *14*, 186. [CrossRef]
20. Chen, Q.; Shi, Y.; Ding, Q.; Ding, W.; Tian, Y. Comparison of straw incorporation effect with down-cut and up-cut rotary tillage. *Trans. Chin. Soc. Agric. Eng.* **2015**, *31*, 13–18. [CrossRef]
21. Guo, J.; Ji, C.; Fang, H.; Zhang, Q.; Hua, F.; Zhang, C. Experimental analysis of soil and Straw displacement after up-cut and down-cut rotary tillage. *Trans. Chin. Soc. Agric. Mach.* **2016**, *47*, 21–26. [CrossRef]
22. Zhang, Z.; He, J.; Li, H.; Wang, Q.; Ju, J.; Yan, X. Design and experiment on straw chopper cum spreader with adjustable spreading device. *Trans. Chin. Soc. Agric. Mach.* **2017**, *48*, 76–87. [CrossRef]
23. Zhao, Y.; Wang, Y.; Liu, H.; Yang, Y.; Gong, Z. Design and Experiment of Stubble-breaking Components on Strip Subsoiling and Stubble-breaking Machine. *Trans. Chin. Soc. Agric. Mach.* **2018**, *49*, 94–103. [CrossRef]
24. Gao, W.; Lin, J.; Li, B.; Ma, T. Parameter optimization and experiment of spiral trenching device for deep buried corn straw returning machine. *Trans. Chin. Soc. Agric. Mach.* **2018**, *49*, 45–54. [CrossRef]
25. Zhang, X.; Li, C.; Li, J.; Zou, M. Vibration characteristic model establishment and experiment of shovel corn precision seeder. *Trans. Chin. Soc. Agric. Mach.* **2014**, *45*, 88–93. [CrossRef]
26. Chen, S.; Zhou, Y.; Tang, Z.; Lu, S. Modal vibration response of rice combine harvester frame under multi-source excitation. *Biosyst. Eng. Biosyst.* **2020**, *194*, 177–195. [CrossRef]
27. Gao, Z.; Xu, L.; Li, Y.; Wang, Y.; Sun, P. Vibration measure and analysis of crawler-type rice and wheat combine harvester in field harvesting condition. *Trans. Chin. Soc. Agric. Eng.* **2017**, *33*, 48–55. [CrossRef]
28. Qian, P.; Lu, T.; Shen, C.; Chen, S. Influence of vibration on the grain flow sensor during the harvest and the difference elimination method. *Int. J. Agric. Biol. Eng.* **2021**, *14*, 149–162. [CrossRef]

29. Pang, J.; Li, Y.; Ji, J.; Xu, L. Vibration excitation identification and control of the cutter of a combine harvester using triaxial accelerometers and partial coherence sorting. *Biosyst. Eng.* **2019**, *185*, 25–34. [CrossRef]
30. Shao, X.; Yang, Z.; Song, Z.; Liu, J.; Yuan, W. Analysis of influence of tractor rotary tillage load on power take-off driveline. *Trans. Chin. Soc. Agric. Mach.* **2022**, *53*, 332–339. [CrossRef]
31. Ma, Z.; Zhang, Z.; Zhang, Z.; Song, Z.; Liu, Y.; Li, Y.; Xu, L. Durable testing and analysis of a cleaning sieve based on vibration and strain signals. *Agriculture* **2023**, *13*, 2232. [CrossRef]
32. Sun, L.; Liu, M.; Wang, Z.; Wang, C.; Luo, F. Research on load spectrum reconstruction method of exhaust system mounting bracket of a hybrid tractor based on MOPSO-Wavelet decomposition technique. *Agriculture* **2023**, *13*, 1919. [CrossRef]
33. Chai, X.; Xu, L.; Sun, Y.; Liang, Z.; Lu, E.; Li, Y. Development of a cleaning fan for a rice combine harvester using computational fluid dynamics and response surface methodology to optimise outlet airflow distribution. *Biosyst. Eng.* **2020**, *192*, 232–244. [CrossRef]
34. Xu, B.; Feng, M.; Tiliwa, E.S.; Yan, W.; Wei, B.; Zhou, C.; Ma, H.; Wang, B.; Chang, L. Multi-frequency power ultrasound green extraction of polyphenols from Pingyin rose: Optimization using the response surface methodology and exploration of the underlying mechanism. *LWT* **2022**, *156*, 113037. [CrossRef]